

Supplement to

Spatiotemporal variability of elemental and organic carbon in Svalbard snow during 2007–2018.

Christian Zdanowicz et al.

Correspondence to: Christian M. Zdanowicz (christian.zdanowicz@geo.uu.se)

EC and OC analyses: Additional information

The C_{snow}^{EC} and C_{snow}^{OC} (ng g⁻¹) in individual snow samples were computed from the filter loadings measured by the TOT method, following:

$$C_{snow}^{EC} = \frac{L_{filt}^{EC} A_{filt}}{V_{meltwater}} \quad (1)$$

$$C_{snow}^{OC} = \frac{L_{filt}^{OC} A_{filt}}{V_{meltwater}} \quad (2)$$

where A_{filt} is the total area of the filter on which particulate matter was collected, and $V_{meltwater}$ the volume of meltwater filtered. Several factors can contribute to uncertainties in the measured particulate carbon loading on filters. These include heterogeneous EC distribution in the snowpack, undercatch during filtration, uneven loading of particles on the filters (shadowing effect; e.g., Cheng et al., 2014), or the pyrolysis of organic compounds which may lead to underestimations of EC relative to OC. The EUSAAR_2 protocol used in the present study is designed to minimize biases due to pyrolysis of OC (Cavalli et al., 2010). For uncertainties in L_{filt}^{EC} arising from snowpack heterogeneity (σ_{sh}) and filtration undercatch (σ_u), we used previous estimates by Forsström et al. (2009, 2013) and Svensson et al. (2013). Comparable information for OC being presently unavailable, we used the same figures of σ_{sh} and σ_u as for EC. The uncertainty arising from uneven filter loading (σ_f) was evaluated from paired measurements on separate 1-cm² filter sections prepared from the April 2016 snow survey samples ($n = 89$). The coefficients of variation (CV) between paired measurements of both L_{filt}^{EC} and L_{filt}^{OC} were found to increase exponentially with the particle mass density on the filters. The median value for L_{filt}^{EC} was 19 % (8 % for L_{filt}^{OC}), with an interquartile range of 7 to 35 % (4 to 19 % for L_{filt}^{OC}). By combining the various sources of error listed above, we estimated a median coefficient of variation (CV) of ~40 % for both C_{snow}^{EC} and C_{snow}^{OC} .

The presence of mineral dust particles on filters can lead to biases in the estimation of L_{filt}^{EC} relative to L_{filt}^{OC} (Wang et al., 2012). Carbonate minerals in particular (e.g., calcite) can release volatile C during the inert atmosphere (He) heating step of thermo-optical analysis, thus introducing a negative bias in L_{filt}^{EC} , and consequently C_{snow}^{EC} (Lim et al., 2014). Published studies suggest that carbonate minerals are only a minor dust constituent in the wintertime aerosol over Svalbard, and thus unlikely to contribute much to deposition in snow (Weinbruch et al., 2012; Moroni et al., 2015). However carbonate rocks outcrop in many areas of Svalbard (e.g., central Spitsbergen, Brøgger Peninsula), are common constituents in some cryosols (4 to 37 % mass; Szymański et al., 2015; Hanaka et al., 2019) and are found in cryoconites on at least some Spitsbergen glaciers (Hodson et al., 2010; Langford et al., 2011). Wind-blown dust deflated from local soils or sediments is therefore a potential source of carbonates and other mineral particles in Svalbard snow. Various correction procedures exist to account for the effect of mineral dust on filters during TOT analysis for EC and OC. These procedures involve HCl fumigation or a thermal-oxidative pre-treatment of filters (Chow et al., 1993; Jankowski et al., 2008; Karansiou et al., 2011). Evangelou et al. (2018) found reductions of 5 to 22 % in the estimated C_{snow}^{EC} after thermal-oxidative pretreatment of snow meltwater filters. However, no pre-treatment was applied to the filters analyzed in the present study, so we cannot quantify biases that may have been introduced by carbonate carbon in C_{snow}^{EC} and C_{snow}^{OC} .

Sampling site	Coordinates (DD° MM.MMM')		Elev. (m a.s.l.)	Sampling date(s)	Snowpack depth (m)	Air T (°C)
	Lat. N	Lon. E				
Lomonosovfonna						
LF1	78° 37.977'	17° 04.600'	223	2016-04-10	0.27	-10.9
LF2*	78° 41.479'	17° 08.991'	523	2016-04-09	0.94	-5.8
LF3*	78° 49.438'	17° 26.085'	1193	2016-04-11	1.46	-24.0
Kongsvegen						
KVG 1	78° 49.808'	12° 45.527'	226	2016-04-13	0.20	-13.9
KVG 1.5	78° 48.773'	12° 52.155'	326	2016-04-13	0.75	-13.9
KVG 2*	78° 46.830'	13° 09.206'	534	2016-04-11	1.62	-17.5
KVG3*	78° 45.335'	13° 20.178'	672	2016-04-12	2.24	-15.5
Holtedahlfonna						
HDF1	78° 55.850'	13° 18.151'	570	2016-04-17	1.10	-14.5
HDF2*	79° 01.762'	12° 31.859'	718	2016-04-17	1.75	-14.2
HDF3*	79° 08.418'	12° 23.653'	1119	2016-04-15	2.34	-18.1
Werenskioldbreen						
WSB1	77° 04.519'	15° 18.797'	166	2016-04-16	0.81	-9.2
WSB2	77° 04.312'	15° 26.435'	413	2016-04-16	1.10	-11.2
WSB3*	77° 05.539'	15° 29.362'	528	2016-04-18	3.30	-11.1
Hansbreen						
HB1	77° 02.917'	15° 38.313'	102	2016-04-25	1.02	-7.3
HB2	77° 04.959'	15° 38.362'	275	2016-04-25	1.69	-6.9
HB3*	77° 07.211'	15° 29.230'	396	2016-04-29	2.88	0.7
Austfonna						
AF1	79° 44.011'	22° 24.853'	336	2016-04-21	1.07	-13.5
AF2*	79° 46.014'	22° 49.485'	507	2016-04-23	1.56	-7.1
AF3*	79° 49.936'	24° 00.265'	785	2016-04-24	1.81	-14.7
Austre Lovénbreen						
ALB1	78° 52.980'	12° 08.133'	195	2016-04-25	0.87	-3.7
ALB2	78° 53.318'	12° 09.552'	340	2016-04-25	1.16	-2.8
ALB3*	78° 51.645'	12° 11.222'	513	2016-04-20	1.61	-11.3
Austre Brøggerbreen	78° 52.422'	11° 55.218'	456	2008-2018	var	var
Sverdrup	78° 55.002'	11° 55.998'	~50	2008-2018	var	var
Gruvebadet	78° 55.050'	11° 53.664'	~50	2008-2018	var	var

Table S1. The principal snow sampling sites for EC and OC analyses presented in this study. An asterisk (*) after the site code identifies snowpit sites for which the snowpack was simulated using the snowpack model (see section 2.4.2). var = variable depending on sampling date.

Sampling site	Coordinates (DD° MM.MMM')		Elev. (m a.s.l.)	Sampling dates(s)	Sampled depth (cm)
	Lat. N	Lon. E			
Austre Lovénbreen					
Top	78° 51.543'	12° 11.843'	513	2016-04-20	0-5
Middle	78° 52.172'	11° 09.002'	340	2016-04-25	0-5
Bottom	78° 53.019'	12° 08.920'	195	2016-04-25	0-5
Midtre Lovénbreen					
Stake 10 (Top)	78° 52.242'	11° 59.016'	403	2017-04-12	0-5
Stake 7 (Middle)	78° 52.590'	12° 01.836'	297	2017-04-12	0-3
Stake 2 (Bottom)	78° 53.604'	12° 03.696'	87	2017-04-12	0-2
Stake 10 (Top)	78° 52.242'	11° 59.016'	403	2017-05-04	0-3
Stake 7 (Middle)	78° 52.590'	12° 01.836'	297	2017-05-04	0-2
Vestre Brøggerbreen					
Bottom	78° 54.708'	11° 44.040'	139	2017-04-09	0-5
Middle	78° 54.234'	11° 39.480'	355	2017-04-11	0-2
Top	78° 53.694'	11° 39.816'	450	2017-04-12	0-2
Bottom	78° 54.708'	11° 44.040'	139	2017-04-12	0-2
Waypoint	78° 54.300'	11° 41.202'	300	2017-04-16	0-8
Edithbreen					
Top	78° 51.180'	11° 11.094'	625	2017-04-13	0-2
Middle	78° 51.276'	11° 45.000'	425	2017-04-13	0-2
Top	78° 51.180'	11° 11.094'	625	2017-04-13	0-2
Holtedahlfonna					
Stake 4	78° 58.667'	13° 28.098'	642	2017-04-11	3-4
Stake 6	79° 01.762'	13° 31.861'	718	2017-04-11	0-3
Kongsvegen					
Stake 8 (Top)	78° 45.334'	13° 20.178'	672	2016-04-12	0-5
Stake 6	78° 46.683'	13° 09.206'	534	2016-04-11	0-5
Stake 3	78° 48.615'	12° 51.263'	326	2016-04-13	0-5
Stake 2 (Bottom)	78° 49.808'	12° 45.527'	226	2016-04-13	0-5
Stake 8 (Top)	78° 45.334'	13° 20.178'	672	2017-04-02	0-5
Stake 6	78° 46.683'	13° 09.206'	534	2017-04-02	0-5
Stake 4	78° 48.167'	12° 57.520'	395	2017-04-02	0-5
Stake 2 (Bottom)	78° 49.808'	12° 45.527'	226	2017-04-02	0-5
Moraine	78° 51.843'	12° 29.460'	3	2017-04-02	0-12
Stake 8 (Top)	78° 45.334'	13° 20.178'	672	2017-04-13	2-4
Stake 6	78° 46.683'	13° 09.206'	534	2017-04-13	0-2
Stake 4	78° 48.167'	12° 57.520'	395	2017-04-13	2-3
Stake 2 (Bottom)	78° 49.808'	12° 45.527'	226	2017-04-13	0-6
Stake 6	78° 46.683'	13° 20.178'	672	2017-05-05	2-6
Stake 6	78° 46.683'	13° 09.206'	534	2017-05-05	0-7

Table S2. Details of additional surface snow sampling sites in northwestern Spitsbergen, 2016–17.

Location	Lat. N	Long. E	Alt. (m.a.s.l.)	Operated by
Hansbreen	77° 02.90'	15° 38.16'	178	University of Silesia
Werenskioldbreen	77° 04.32'	15° 26.40'	358	University of Silesia
Nordenskiöldbreen	78° 44.39'	17° 19.87'	685	Uppsala & Utrecht Universities
Kongsvegen	78° 46.82'	13° 09.61'	534	Norwegian Polar Institute (NPI)
Holtedalfonna	78° 59.00'	13° 36.99'	692	Norwegian Polar Institute (NPI)
Etonbreen/Austfonna	79° 43.97'	22° 25.01'	369	University of Oslo & NPI

Table S3. Automated Weather Stations (AWS) from which supporting data were obtained for this study.

Site (<i>landscape type</i>)	Year(s) of sampling	Thermal protocol	Data source
Summit, central Greenland (<i>glacier</i>)	2005	NIOSH 5040	Hagler et al. (2007)
Svalbard: Holtedahlfonna (<i>glacier</i>)	2006 to 2014	EUSAAR-2	Ruppel et al. (2017)
Svalbard (<i>glaciers, sea ice, tundra</i>)	2007	NIOSH 5040	Forsström et al. (2009)
Svalbard (<i>glaciers, sea ice, tundra</i>)	2008	NIOSH 5040	Aamaas et al. (2011)
Svalbard (<i>glaciers, sea ice, tundra</i>)	2007 to 2009	EUSAAR-2	Forsström et al. (2013)
Northern Scandinavia (<i>forest, treeline, tundra</i>)	2007 to 2009	EUSAAR-2	Forsström et al. (2013)
Northern Sweden (<i>rural, forested/tundra</i>)	2017	EUSAAR-2	Unpublished data, Table S4
Northern Finland (<i>rural, forest</i>)	2009 to 2011	NIOSH 5040	Meinander et al. (2013)
Northern Finland (<i>rural, forest</i>)	2010	NIOSH 5040	Svensson et al. (2013)
Northern Finland rural, (<i>forest</i>)	2013 to 2016	EUSAAR-2	Svensson et al. (2018)
NW Siberia and NW Russia (<i>rural, forest, tundra</i>)	2014 to 2016	EUSARR-2	Evangelou et al. (2018)
Barrow, coastal Alaska (<i>tundra</i>)	2015	DRI	Dou et al. (2017)
St. Elias Mountains, Yukon, Canada (<i>glacier</i>)	2016	EUSAAR-2	Unpublished data, Table S4

Table S4. Details of the C_{snow}^{EC} data presented on **Fig. 11**. Methodological details are given in these publications: NIOSH 5040: Birch and Cary (1996); EUSAAR-2: Cavalli et al. (2010); DRI: Chow et al. (1993). The C_{snow}^{EC} measured by the NIOSH 5040 protocol were multiplied by a factor of 2, as in Forsström et al. (2013).

Location	Coordinates (DD° MM.MMM')		Alt.	Year	Month	Day	C_{snow}^{OC} (ng g ⁻¹)	C_{snow}^{EC} (ng g ⁻¹)	Depth (cm)	n
	Latitude	Longitude	(m)							

(Rural, forested or remote sites)

Gällivare	N 67° 09.187'	E 20° 43.379'	326	2014	4	4	592.1	29.9	98	2
Abisko	N 68° 21.818'	E 18° 45.751'	427	2014	4	5	872.8	22.6	75	1
Arvidsjaur	N 65° 34.427'	E 19° 13.344'	390	2014	4	6	690.2	35.5	64	2
Jokkmokk	N 66° 36.340'	E 19° 46.756'	272	2014	4	6	594.8	29.4	69	2
Puoltisvaara	N 67° 26.294'	E 21° 06.075'	383	2014	4	6	440.9	22.2	70	2
Lycksele	N 64° 36.248'	E 18° 43.652'	268	2014	4	7	420.0	52.4	65	2
Svartberget	N 64° 15.354'	E 19° 47.041'	258	2014	4	7	952.2	44.9	78	2

(Core drilled on mountain icefield on 15 May, 2016. Years shown are estimates)

Eclipse Icefield	N 60° 50.088'	W 139° 49.746'	3020	2016			1050.2	10.4	0-150	3
Eclipse Icefield	N 60° 50.088'	W 139° 49.746'	3020	2015			229.5	3.3	150-350	3
Eclipse Icefield	N 60° 50.088'	W 139° 49.746'	3020	2014			161.8	3.4	350-700	7
Eclipse Icefield	N 60° 50.088'	W 139° 49.746'	3020	2013			173.3	2.9	700-1000	6
Eclipse Icefield	N 60° 50.088'	W 139° 49.746'	3020	2012			183.1	3.8	1000-1200	6
Eclipse Icefield	N 60° 50.088'	W 139° 49.746'	3020	2011			183.1	3.3	1200-1500	5
Eclipse Icefield	N 60° 50.088'	W 139° 49.746'	3020	2010			138.9	3.4	1550-1650	4
Eclipse Icefield	N 60° 50.088'	W 139° 49.746'	3020	2009			138.2	1.5	1650-1720	1

Table S5. C_{snow}^{EC} and C_{snow}^{OC} from Sweden and the Yukon used for comparison on Fig. 11. These data were collected during reconnaissance surveys in 2014 and 2016, and were handled and analyzed by the same methods and protocols described for the Svalbard data. The samples from Sweden were recovered with assistance from M. Syk and J. Vollmer, Uppsala University, and the Eclipse Icefield core by K. Kreutz, University of Maine, USA.

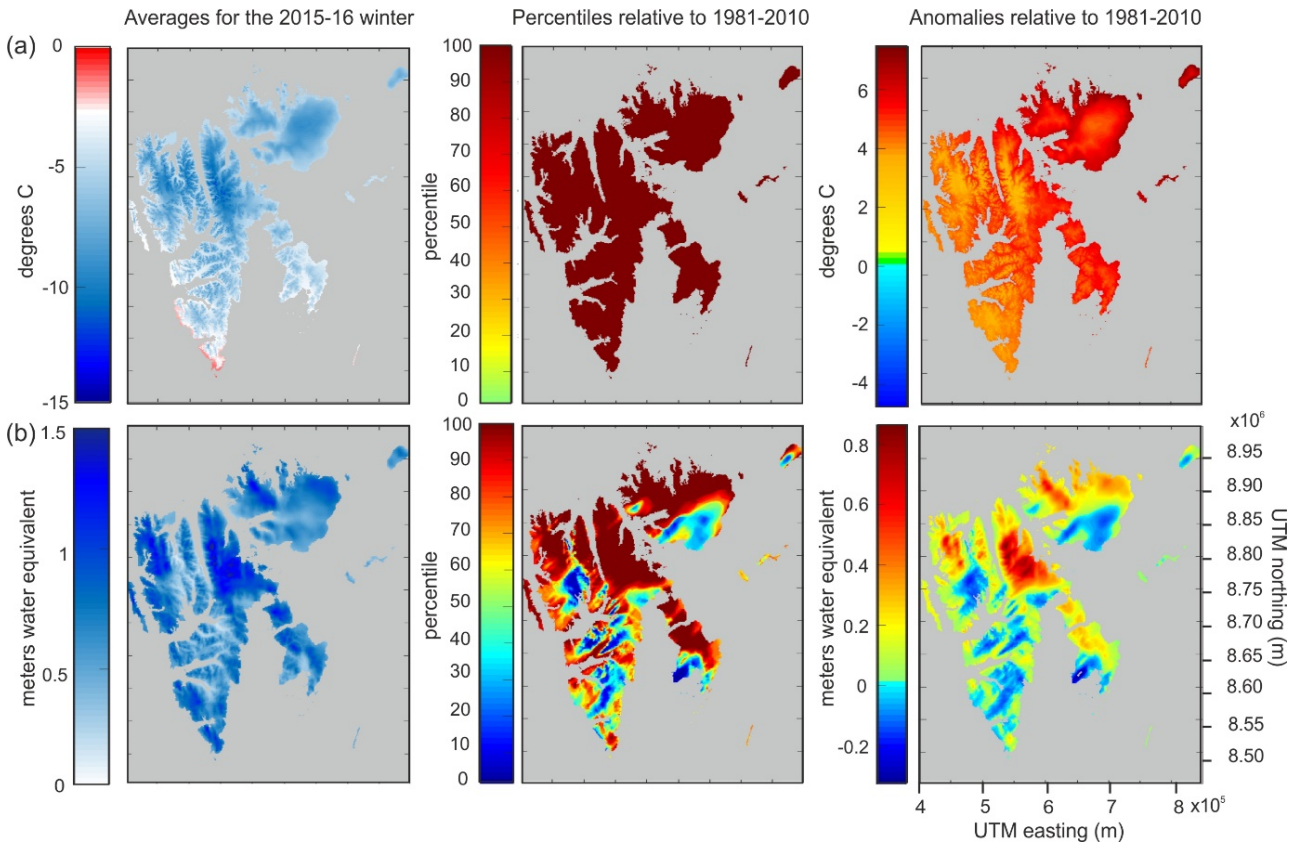


Fig. S1. Comparison of (a) mean surface temperatures and (b) total precipitation (snow + rainfall) over Svalbard during the winter 2015–16 (1 Oct 2015 to 30 April 2016) from gridded ERA Interim reanalysis data fields. Left: Mean winter temperature or total precipitation across the archipelago. Centre: Percentile ranking for the winter 2015–16, when compared to the cumulative probability distributions of these conditions during the 30-year climatological reference period 1981–2010. Right: Mean anomalies of temperature or total precipitation in the winter 2015–16 when compared to the climatology of the 1981–2010 period.



Fig. S2. Southward-looking perspective view over part of Brøgger Peninsula, northwestern Spitsbergen, showing the snow sampling sites in this area in relation to Ny-Ålesund and the Zeppelin Observatory. The elevation of some high peaks (m a.s.l.) is shown to provide a vertical scale reference. Image generated with the online mapping service of the Norwegian Polar Institute (<https://toposvalbard.npolar.no/>)

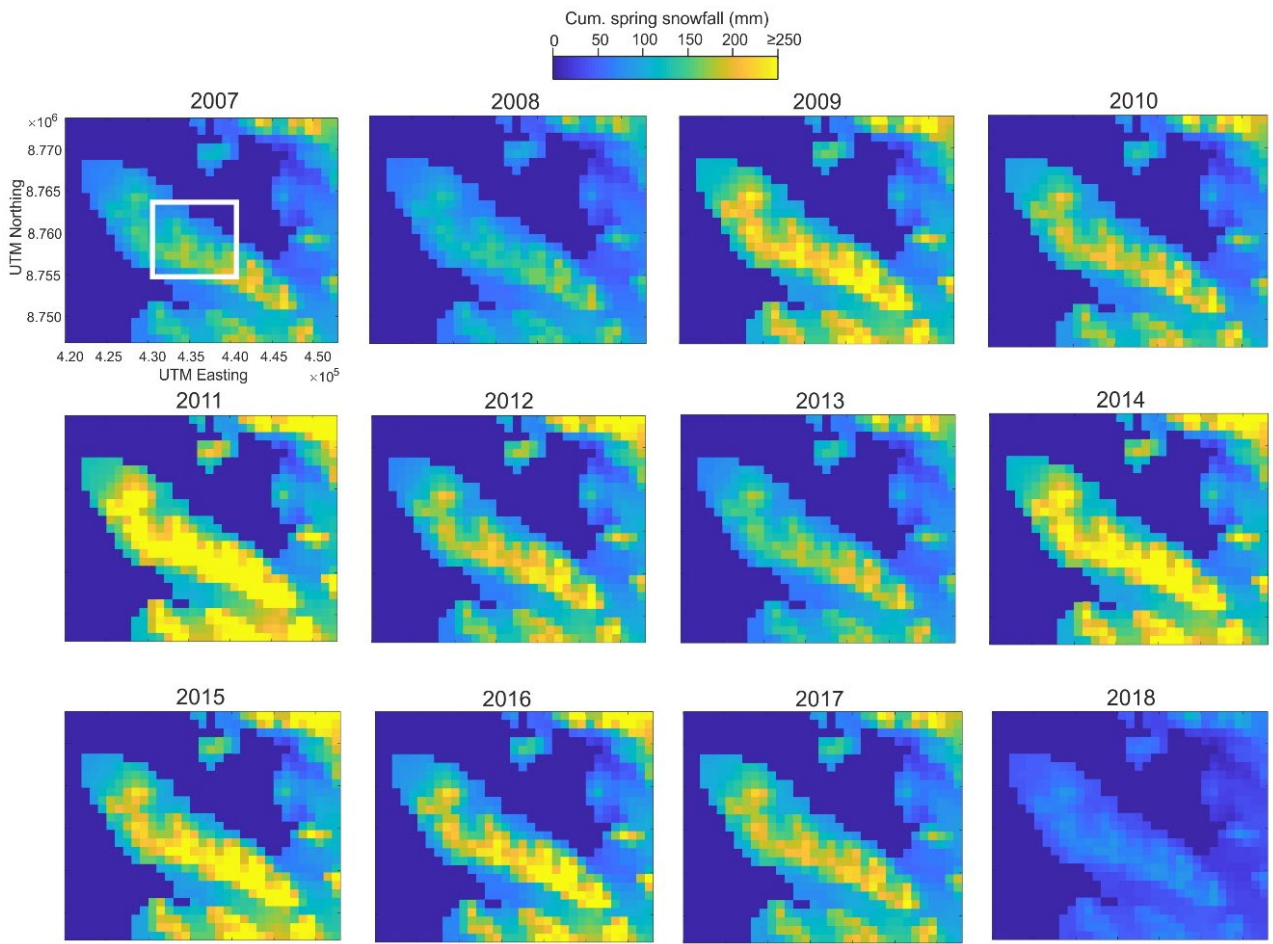


Fig. S3. Cumulative spring snowfall (March-April-May) over Brøgger Peninsula between 2007 and 2018, simulated with a snowpack model ([van Pelt et al., 2019](#)). The grid cell size is 10 x 10 km. The white frame on the first panel (2007) corresponds approximately to the area shown on **Fig. S2**.

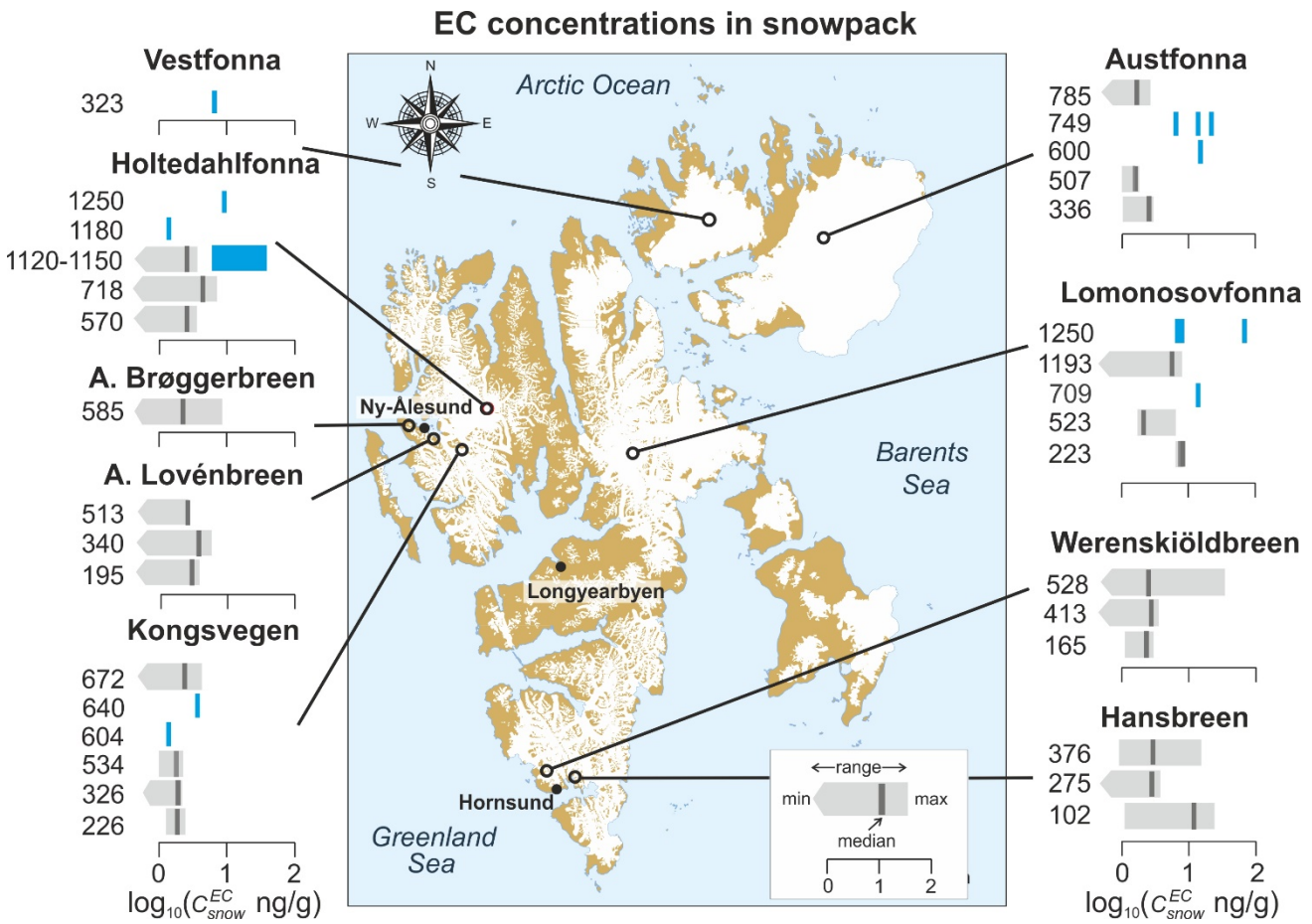


Fig. S4. $C_{\text{snow}}^{\text{EC}}$ on glaciers across Svalbard. For each site, sub-plots correspond to different elevations, which are specified to the left of each plot, in meters a.s.l.. The $C_{\text{snow}}^{\text{EC}}$ data shown in grey are from the April 2016 survey, or from annual monitoring on Austre Brøggerbreen ($C_{\text{snow}}^{\text{EC}}$ values for 2007–18). The data in blue include $C_{\text{snow}}^{\text{EC}}$ from the 2007–09 surveys reported by Forsström et al. (2009, 2013), and the range of $C_{\text{snow}}^{\text{EC}}$ on Holtedahlfonna over the period 2006–14, after Ruppel et al. (2017).

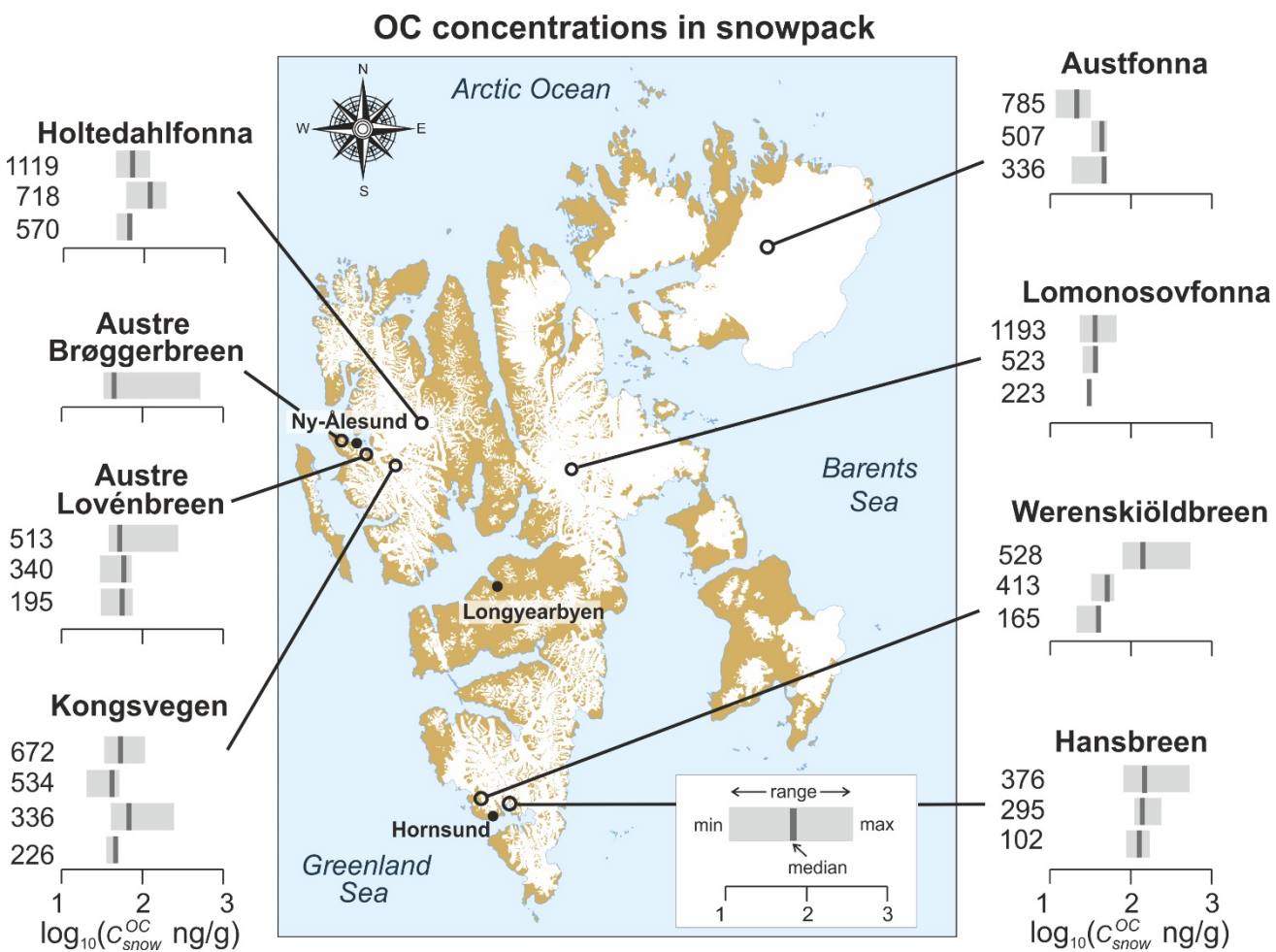


Fig. S5. As in **Fig. S4**, but for $C_{\text{snow}}^{\text{OC}}$.

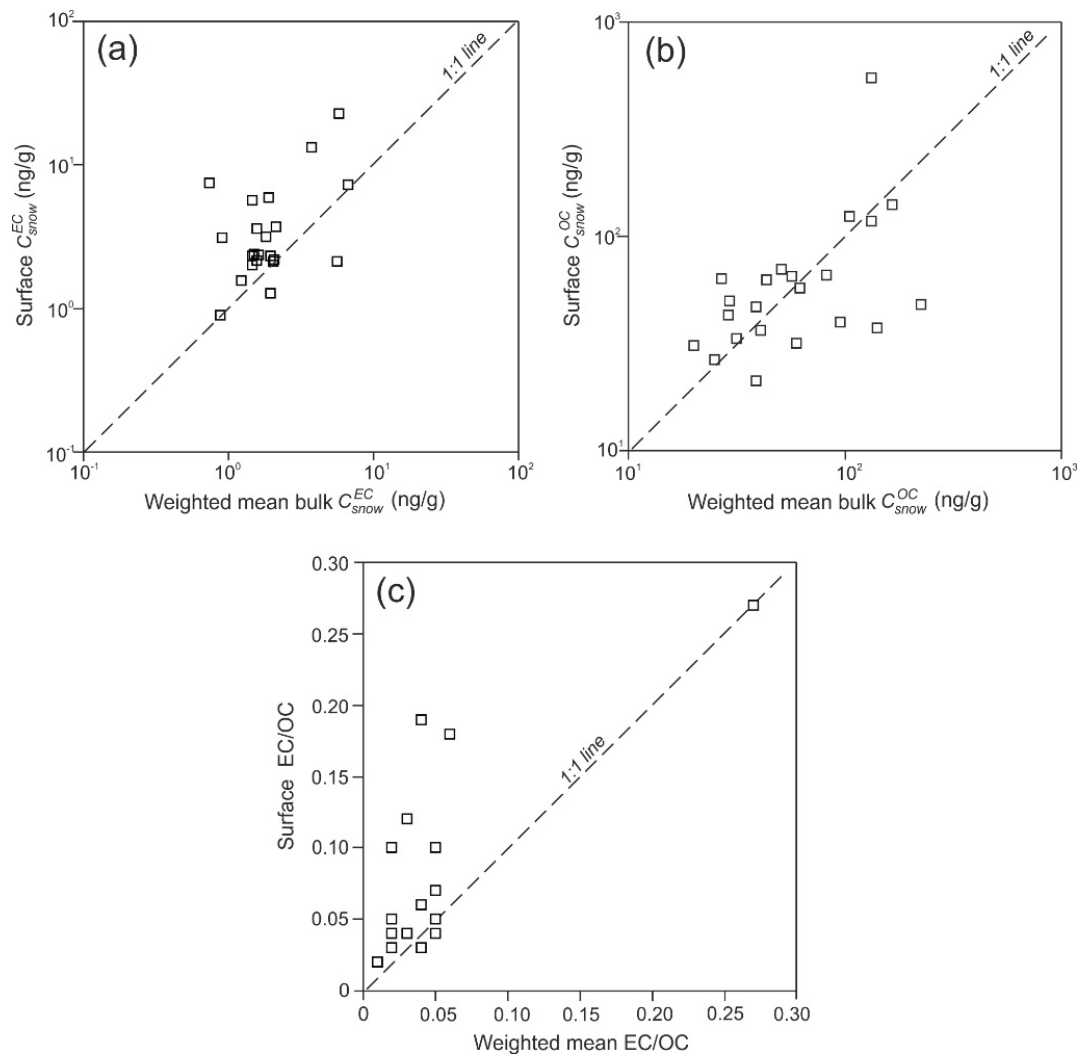


Fig. S6. (a) $C_{\text{snow}}^{\text{EC}}$, (b) $C_{\text{snow}}^{\text{OC}}$ and (c) EC/OC in surface vs. bulk snowpack layers on Svalbard glaciers.

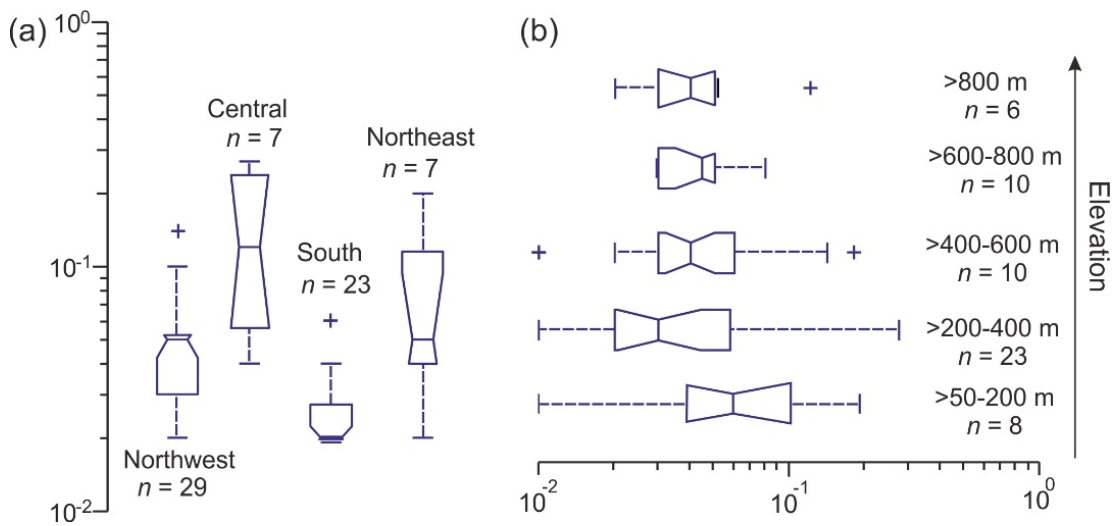


Fig. S7. Variations in EC/OC in the snow samples collected during the April 2016 glacier survey across Svalbard. Data are shown by (a) geographic sector and (b) altitude bins, as in **Fig. 3 and 4**. Values of $C_{\text{snow}}^{\text{EC}}$ or $C_{\text{snow}}^{\text{OC}} < 1 \text{ ng g}^{-1}$ were excluded when computing EC/OC.

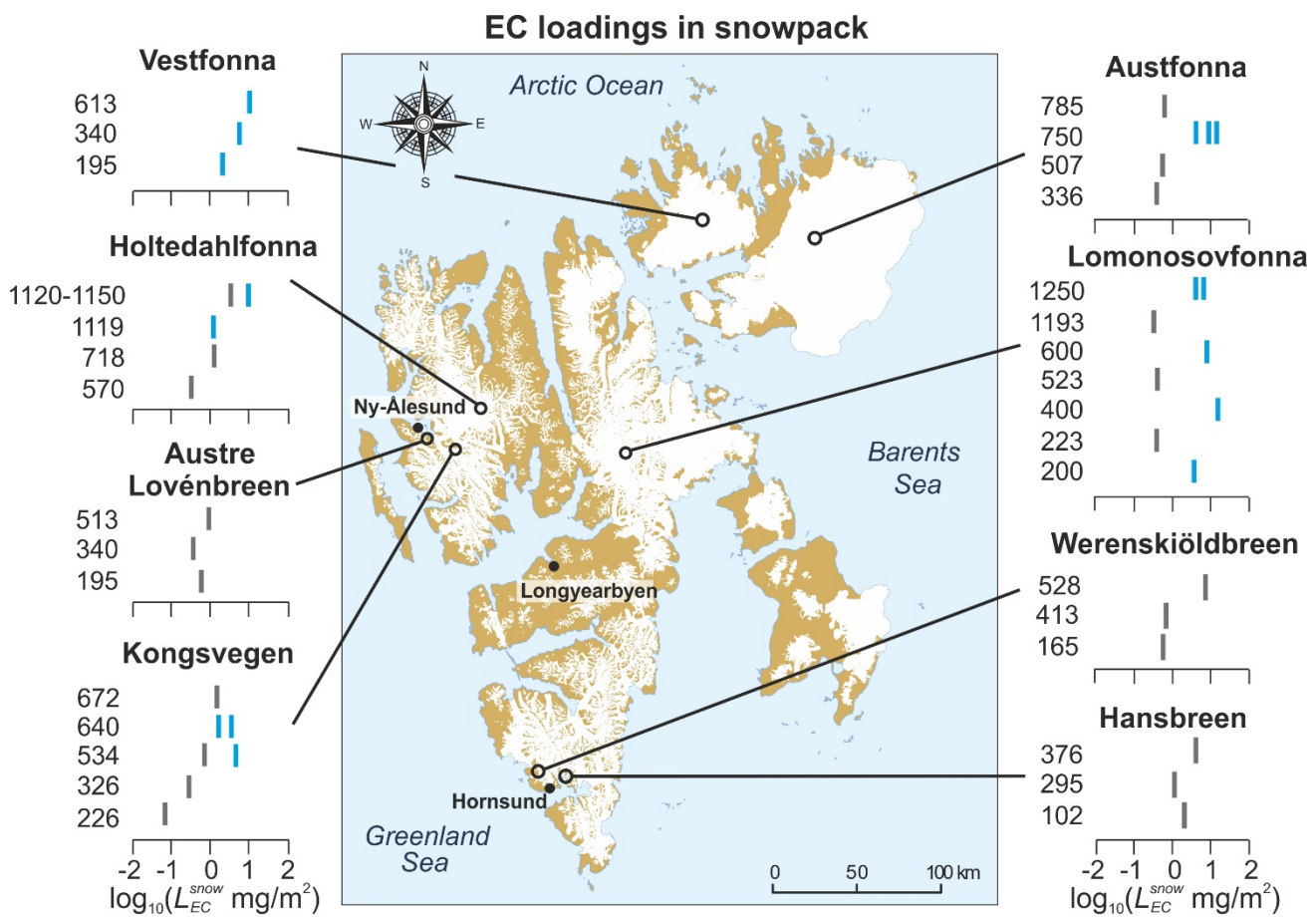


Fig. S8. $L_{\text{snow}}^{\text{EC}}$ on glaciers across Svalbard. Colors are as defined in **Fig. S4**. The blue marker at Holdedahlfonna summit (1120–50 m a.s.l.) is the calculated mean annual $L_{\text{snow}}^{\text{EC}}$ at this site from snow and firn data spanning an estimated 8 years (2006–14; Ruppel et al., 2017). The mean $L_{\text{snow}}^{\text{EC}}$ in the late winter snowpack could be less than half of this value.

OC loadings in snowpack

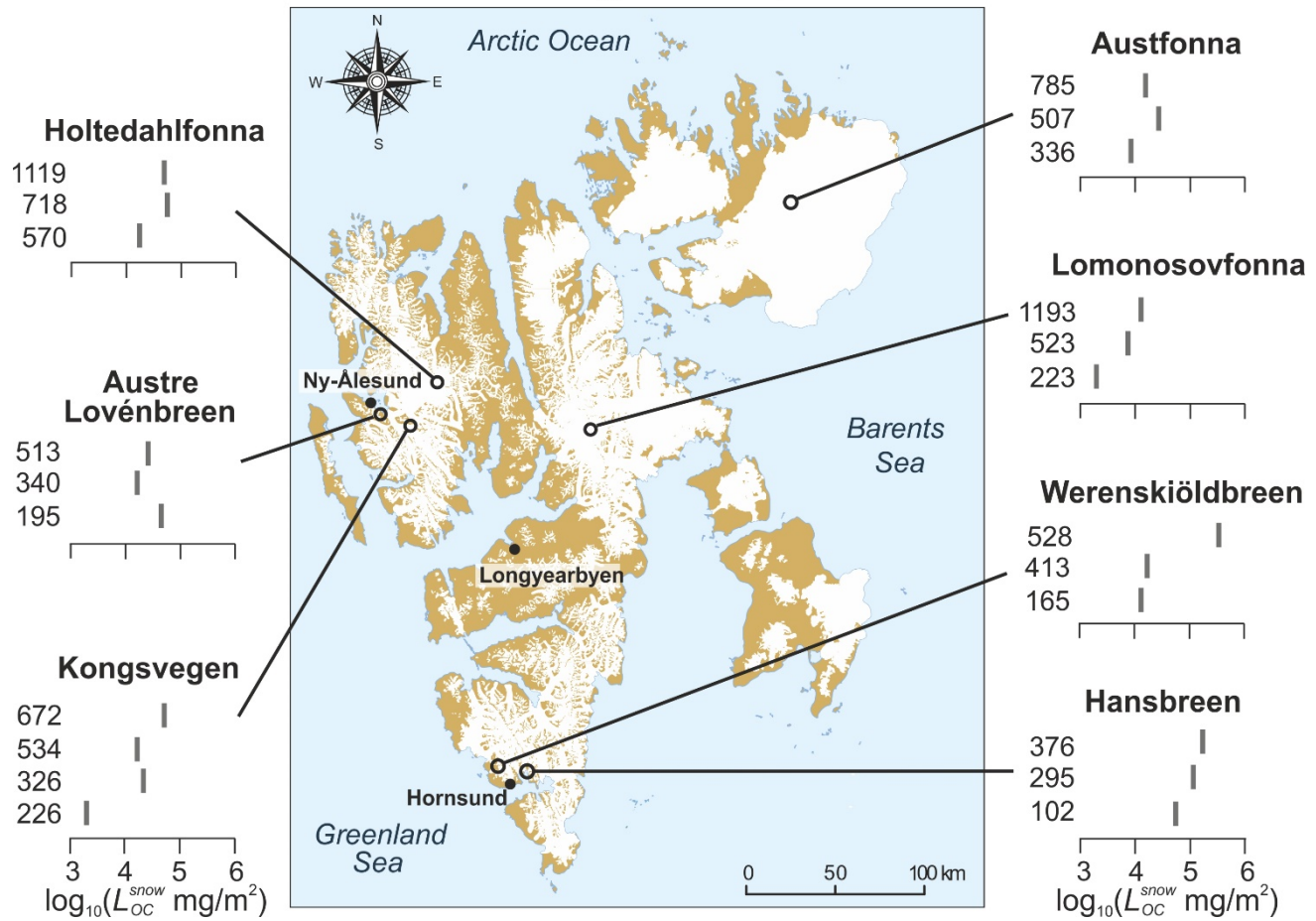


Fig. S9. As in **Fig. S8**, but for L_{OC}^{snow} .

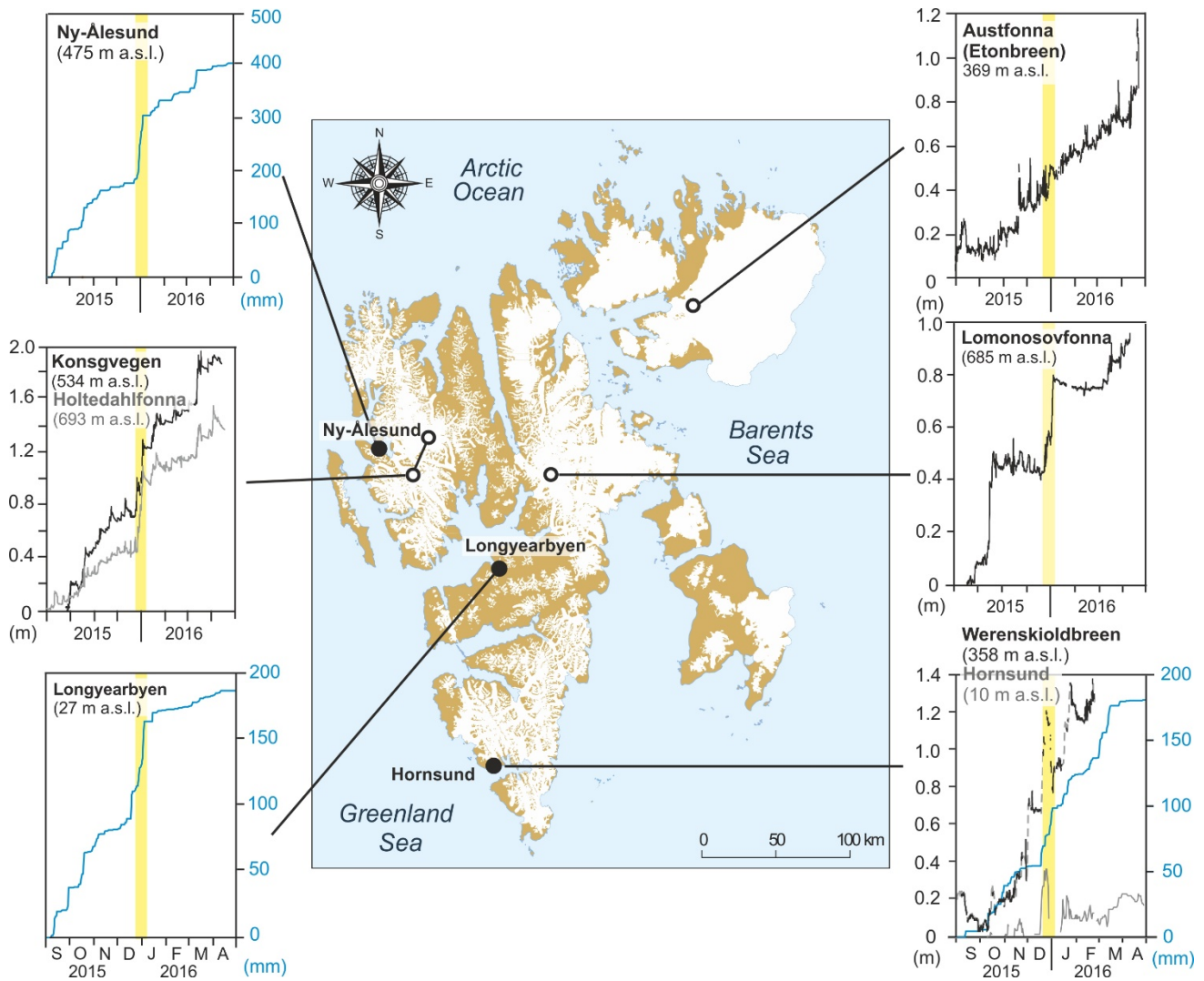


Fig. S10. The signature of the late December 2015 snowstorm (highlighted) across Svalbard. Black/grey: Changes in snowpack thickness or relative surface height (left-hand scale, in m); Blue: cumulative precipitation (right-hand scale, in mm w.e.). Data from glaciers come from the automated weather stations (**Table S3**), while other data are from weather stations at Longyearbyen, the airport in Ny-Ålesund, and from the Polish Polar Station Hornsund.

References

- Aamaas, B., Bøggild, C.E., Stordal, F., Berntsen, T., Holmén, K. and Ström, J.: Elemental carbon deposition to Svalbard snow from Norwegian settlements and long-range transport, *Tellus*, 63B, 340–351, doi:10.1111/j.1600-0889.2011.00531.x, 2011.
- Birch, M.E. and Cary, R.A.: Elemental carbon-based method for monitoring occupational exposures to particulate diesel exhaust. *Aerosol Sci. Technol.* 25, 221–241, doi:10.1080/10473220290035390, 1996.
- Dou, T., Xiao, C., Du, Z., Schauer, J.J., Ren, H., Ge, B., Xie, A., Tan, J., Fu, P. and Zhang, Y.: Sources, evolution and impacts of EC and OC in snow on sea ice: a measurement study in Barrow, Alaska, *Sci. Bull.* 62, 1547–1554, doi:10.1016/j.scib.2017.10.014, 2017.
- Cavalli, F., Viana, M., Yttri, K. E., Genberg, J., and Putaud, J.-P.: Toward a standardised thermal-optical protocol for measuring atmospheric organic and elemental carbon: the EUSAAR protocol, *Atmos. Meas. Tech.*, 3, 79–89, doi:10.5194/amt-3-79-2010, 2010.
- Cheng, Y., Hea, K.-B., Duana, F.-K., Du, Z.-L., Zheng, M. and Ma, Y.-L.: Ambient organic carbon to elemental carbon ratios: Influence of the thermal–optical temperature protocol and implications, *Sci. Tot. Environ.*, 468–469, 1103–1111, doi:10.1016/j.scitotenv.2013.08.084, 2014.
- Chow, J.C., Watson, J.G., Pritchett, L.C., Rierson, W.R., Frazier, C.A. and Purcell, R.G.: The DRI thermal/optical reflectance carbon analysis system: description, evaluation and applications in U.S. Air quality studies, *Atmos. Environ.* 27, 8, 1185–1201, doi:10.1016/0960-1686(93)90245-T, 1993.
- Evangelou, N., Shevchenko, V. P., Yttri, K. E., Eckhardt, S., Sollum, E., Pokrovsky, O. S., Kobelev, V. O., Korobov, V. B., Lobanov, A. A., Starodymova, D. P., Vorobiev, S. N., Thompson, R. L., and Stohl, A.: Origin of elemental carbon in snow from western Siberia and northwestern European Russia during winter–spring 2014, 2015 and 2016, *Atmos. Chem. Phys.*, 18, 963–977, doi:10.5194/acp-18-963-2018, 2018.
- Forsström, S., Isaksson, E., Skeie, R. B., Ström, J., Pedersen, C. A., Hudson, S. R., Berntsen, T. K., Lihavainen, H., Godtliebsen, F. and Gerland, S. : Elemental carbon measurements in European Arctic snow packs, *J. Geophys. Res. Atmos.*, 118, 13,614–13,627, doi:10.1002/2013JD019886, 2013.
- Forsström, S., Ström, J., Pedersen, J. C. A., Isaksson, E., and Gerland, S.: Elemental carbon distribution in Svalbard snow, *J. Geophys. Res. Atmos.* 114, D19112, doi:10.1029/2008JD011480, 2009.
- Hagler, G. S. W., Bergin, M.H., Smith, E.A., Dibb, J.E., Anderson, C. and Steig, E.J.: Particulate and water-soluble carbon measured in recent snow at Summit, Greenland, *Geophys. Res. Lett.*, 34, L16505, doi:10.1029/2007GL030110, 2007.
- Hanaka, A., Plak, A., Zagórski, P., Ozimek, E., Rysiak, A., Majewska, M., and Jaroszuk-Ścisł, J.: Relationships between the properties of Spitsbergen soil, number and biodiversity of rhizosphere microorganisms, and heavy metal concentration in selected plant species, *Plant Soil*, 436, 49–69, doi:10.1007/s11104-018-3871-7, 2019.
- Hodson, A., Cameron, K., Bøggild, C., Irvine-Fynn, T., Langford, H., Pearce, D., and Banwart, S.: The structure, biological activity and biogeochemistry of cryoconite aggregates upon an Arctic valley glacier: Longyearbreen, Svalbard, *J. Glaciol.*, 56, 196, 349–362, doi: 10.3189/002214310791968403, 2010.
- Jankowski, N., Schmidl, C., Marr, I.L., Bauer, H. and Puxbaum, H.: Comparison of methods for the quantification of carbonate carbon in atmospheric PM10 aerosol samples, *Atmos. Environ.*, 42, 8055–8064, doi:10.1016/j.atmosenv.2008.06.012, 2008.
- Karanasiou, A., Diapouli, E., Cavalli, F., Eleftheriadis, K., Viana, M., Alastuey, A., Querol, X. and Reche, C.: On the quantification of atmospheric carbonate carbon by thermal/optical analysis protocols, *Atmos. Meas. Tech.*, 4(11), 2409–2419, doi:10.5194/amt-4-2409-2011, 2011.

- Langford, H., Hodson, A. and Banwart, S.: Using FTIR spectroscopy to characterise the soil mineralogy and geochemistry of cryoconite from Aldegondabreen glacier, Svalbard, *Appl. Geochem.*, 26, S206–S209, doi:10.1016/j.apgeochem.2011.03.105, 2011.
- Lim, S., Faïn, X., Zanatta, M., Cozic, J., Jaffrezo, J.-L., Ginot, P., and Laj, P.: Refractory black carbon mass concentrations in snow and ice: method evaluation and inter-comparison with elemental carbon measurement, *Atmos. Meas. Tech.*, 7, 3307–3324, doi:10.5194/amt-7-3307-2014, 2014.
- Moroni, B., Becagli, S., Bolzacchini, E., Busetto, M., Cappelletti, D., Crocchianti, S., Ferrero, L., Frosini, D., Lanconelli, C., Lupi, A., Maturilli, M., Mazzola, M., Perrone, M.G., Sangiorgi, G., Traversi, R., Udisti, R., Viola, A. and Vitale, V.: Vertical profiles and chemical properties of aerosol particles upon Ny-Ålesund (Svalbard islands), *Adv. Meteorol.*, 2015, 292081, doi:10.1155/2015/292081, 2015.
- Ruppel, M. M. Soares, J., Gallet, J.-C., Isaksson, E., Martma, T., Svensson, J., Kohler, J., Pedersen, C.A., Manninen, S., Korhola, A. and Strömgren, J.: Do contemporary (1980–2015) emissions determine the elemental carbon deposition trend at Holtedahlfonna glacier, Svalbard? *Atmos. Chem. Phys.*, 17, 12,779–12,795, doi:10.5194/acp-17-12779-2017, 2017.
- Meinander, O., Kazadzis, S., Arola, A., Riihelä, A., Räisänen, P., Kivi, R., Kontu, A., Kouznetsov, R., Sofiev, M., Svensson, J., Suokanerva, H., Aaltonen, V., Manninen, T., Roujean, J.-L., and Hautecoeur, O.: Spectral albedo of seasonal snow during intensive melt period at Sodankylä, beyond the Arctic Circle, *Atmos. Chem. Phys.*, 13, 3793–3810, doi:10.5194/acp-13-3793-2013, 2013.
- Svensson, J., Strömgren, J., Kivekäs, N., Dkhar, N. B., Tayal, S., Sharma, V. P., Jutila, A., Backman, J., Virkkula, A., Ruppel, M., Hyvärinen, A., Kontu, A., Hannula, H.-R., Leppäranta, M., Hooda, R. K., Korhola, A., Asmi, E., and Lihavainen, H.: Light-absorption of dust and elemental carbon in snow in the Indian Himalayas and the Finnish Arctic, *Atmos. Meas. Tech.*, 11, 1403–1416, doi:10.5194/amt-11-1403-2018, 2018.
- Svensson, J., Strömgren, J., Hansson, M., Lihavainen, H., and Kerminen, V.-M.: Observed metre scale horizontal variability of elemental carbon in surface snow, *Environ. Res. Lett.*, 8, 034012, doi:10.1088/1748-9326/8/3/034012, 2013.
- Szymański, W., Skiba, M., Wojtuń, B., and Drewnik, M.: Soil properties, micromorphology, and mineralogy of cryosols from sorted and unsorted patterned grounds in the Hornsund area, SW Spitsbergen, *Geoderma*, 253–254, 1–11, doi: 10.1016/j.geoderma.2015.03.029, 2015.
- Van Pelt, W., Pohjola, V., Pettersson, R., Marchenko, S., Kohler, J., Luks, B., Ove Hagen, J.O., Schuler, T.V., Dunse, T., Noël, B. and Reijmer, C.: A long-term dataset of climatic mass balance, snow conditions, and runoff in Svalbard (1957–2018), *The Cryosphere*, 13, 2259–2280, doi:10.5194/tc-13-2259-2019, 2019.
- Wang, M., Xu, B., Zhao, H., Cao, J., Joswiak, D., Wu, G. and Lin, S.: The influence of dust on quantitative measurements of black carbon in ice and snow when using a thermal optical method, *Aerosol Sci. Tech.*, 46, 1, 60–69, doi:10.1080/02786826.2011.605815, 2012.
- Weinbruch, S., Wiesemann, D., Ebert, M., Schütze, K., Kallenborn, R. and Strömgren, J.: Chemical composition and sources of aerosol particles at Zeppelin Mountain (Ny-Ålesund, Svalbard): An electron microscopy study, *Atmos. Environ.*, 49, 142–150, doi:10.1016/j.atmosenv.2011.12.008, 2012.